

# Selective induction of chemotherapy resistance of mammary tumors in a conditional mouse model for hereditary breast cancer

Sven Rottenberg<sup>†</sup>, Anders O. H. Nygren<sup>‡</sup>, Marina Pajic<sup>†</sup>, Fijs W. B. van Leeuwen<sup>§</sup>, Ingrid van der Heijden<sup>†</sup>, Koen van de Wetering<sup>†</sup>, Xiaoling Liu<sup>†</sup>, Karin E. de Visser<sup>†</sup>, Kenneth G. Gilhuijs<sup>§</sup>, Olaf van Tellingen<sup>§</sup>, Jan P. Schouten<sup>‡</sup>, Jos Jonkers<sup>†</sup>, and Piet Borst<sup>†¶</sup>

<sup>†</sup>Division of Molecular Biology and Center of Biomedical Genetics and <sup>§</sup>Division of Diagnostic Oncology, The Netherlands Cancer Institute, 1066 CX Amsterdam, The Netherlands; and <sup>‡</sup>MRC-Holland BV, 1057 SN Amsterdam, The Netherlands

Edited by Inder M. Verma, The Salk Institute for Biological Studies, La Jolla, CA, and approved June 1, 2007 (received for review March 30, 2007)

We have studied *in vivo* responses of “spontaneous” *Brca1*- and *p53*-deficient mammary tumors arising in conditional mouse mutants to treatment with doxorubicin, docetaxel, or cisplatin. Like human tumors, the response of individual mouse tumors varies, but eventually they all become resistant to the maximum tolerable dose of doxorubicin or docetaxel. The tumors also respond well to cisplatin but do not become resistant, even after multiple treatments in which tumors appear to regrow from a small fraction of surviving cells. Classical biochemical resistance mechanisms, such as up-regulated drug transporters, appear to be responsible for doxorubicin resistance, rather than alterations in drug-damage effector pathways. Our results underline the promise of these mouse tumors for the study of tumor-initiating cells and of drug therapy of human cancer.

multidrug resistance | P-glycoprotein | cancer stem cells

Treatment of metastatic cancer often fails in the end, because tumors are resistant to all drugs available. Understanding the mechanisms of resistance may therefore lead to improved treatment. Analysis of tumor samples from patients and of tumor cell lines selected for resistance *in vitro* has led to the identification of a wide range of resistance mechanisms (1, 2). In cases where the drug target is altered, the clinical relevance of the identified resistance mechanism is often unambiguous. A good example is resistance to imatinib (Gleevec), which targets the activated Abelson tyrosine kinase. Alterations in the amino acid sequence of the kinase can fully explain resistance in patients with chronic myeloid leukemia (3). For other drugs, the cause of resistance in patients is not always clear. Examples are the natural product drugs that enter cells by passive diffusion. These include major anticancer drugs, such as *vinca* alkaloids and taxanes, which target tubulin; and the anthracyclines and epipodophyllotoxins (etoposide), which target topoisomerase II (4). These drugs are affected not only by target alterations but also by drug transporters, such as P-glycoprotein, that transport the drug out of the cell before it can reach its target (2). Because induction of apoptosis/senescence is one of the ways in which drugs kill cells, resistance to apoptosis/senescence can also affect the action of these drugs (5–7). In addition, drug effectiveness can be decreased by other tumor properties, e.g., noncycling cells, poor penetration of drug into the tumor because of increased intratumor fluid pressure, etc. (4, 8). How little is known is illustrated by the ongoing discussion of the relevance of drug transporters vs. apoptosis resistance in explaining multidrug resistance against natural product drugs (9–15).

Dissecting the relative importance of each of these resistance mechanisms *in vivo* has been difficult, because realistic animal models for drug resistance are lacking. We have therefore tested whether the newer mouse tumor models, which develop “spontaneous” tumors as a consequence of conditional tissue-specific mutations in protooncogenes/tumor suppressor genes (16), are more suitable for studying resistance *in vivo*. We show here that resistance to the maximum tolerable dose (MTD) of doxorubicin or

docetaxel is readily and reproducibly obtained in mammary tumors arising in mice with conditionally mutated *p53* and *Brca1* tumor suppressor genes.

## Results

**Spontaneous *Brca1*<sup>-/-</sup>;*p53*<sup>-/-</sup> Mouse Mammary Tumors Acquire Complete Resistance to Doxorubicin or Docetaxel but Not to Cisplatin.** To investigate the development of chemotherapy resistance of sporadic mouse tumors, we chose the *K14cre;Brca1*<sup>F/F</sup>;*p53*<sup>F/F</sup> mouse model for hereditary breast cancer, because it shares key morphologic and molecular features with BRCA1-associated breast cancer in humans (17). Moreover, the tumors are relatively superficial and therefore accessible for sizing and biopsy sampling. As anticancer drugs, we selected the anthracycline doxorubicin and the taxane docetaxel, which are both frequently used in the clinic to treat breast cancer. In addition, we included the DNA-adduct-forming drug cisplatin, because of its enhanced *in vitro* cytotoxicity in BRCA1-deficient cells (18, 19). For each of these drugs, we established the MTD based on animal weight loss to mimic a clinically relevant drug concentration [supporting information (SI) Fig. 5]. The mice required a minimal recovery time of 10 days after doxorubicin administration (5 mg/kg), 20 days after cisplatin (6 mg/kg), and 7 days after docetaxel (25 mg/kg). In comparison, WT animals of the same genetic background recovered 7 days after the same dose of doxorubicin and tolerated an additional dose of cisplatin on day 6. No significant difference was seen between mutant and WT mice for docetaxel (data not shown). Mammary tumors arise in *K14cre;Brca1*<sup>F/F</sup>;*p53*<sup>F/F</sup> female mice after a mean latency of ≈213 days. When the tumors were ≈200 mm<sup>3</sup> [volume (*V*) = 0.5 × length × width<sup>2</sup>], we took tumor biopsies using a 15-gauge trocar. Subsequently, the mice were either left untreated (Fig. 1*B*) or treated with 5 mg of doxorubicin, 25 mg of docetaxel, or 6 mg of cisplatin per kilogram (Fig. 1*C*). In nontreated animals, tumors grew rapidly to a size of ≈1,500 mm<sup>3</sup> within ≈10 days. Doxorubicin or docetaxel administration inhibited tumor growth, but there were

Author contributions: S.R., A.O.H.N., M.P., F.W.B.v.L., O.v.T., J.P.S., J.J., and P.B. designed research; S.R., A.O.H.N., M.P., F.W.B.v.L., I.v.d.H., K.v.d.W., X.L., K.E.d.V., and O.v.T. performed research; S.R., A.O.H.N., M.P., F.W.B.v.L., I.v.d.H., K.G.G., J.J., and P.B. analyzed data; and S.R., J.J., and P.B. wrote the paper.

Conflict of interest statement: A.O.H.N. and J.P.S. are employees of MRC-Holland BV, which markets the MLPA test used in this paper.

This article is a PNAS Direct Submission.

Freely available online through the PNAS open access option.

Abbreviations: MTD, maximum tolerable dose; SAM, significance analysis of microarrays; RT-MPLA, reverse transcriptase-multiplex ligation-dependent probe amplification.

Data deposition: The microarray data reported in this paper have been deposited in the Array Express database, [www.ebi.ac.uk/arrayexpress](http://www.ebi.ac.uk/arrayexpress) (accession no. E-NCMF-5).

<sup>¶</sup>To whom correspondence should be addressed. E-mail: p.borst@nki.nl.

This article contains supporting information online at [www.pnas.org/cgi/content/full/0702955104/DC1](http://www.pnas.org/cgi/content/full/0702955104/DC1).

© 2007 by The National Academy of Sciences of the USA

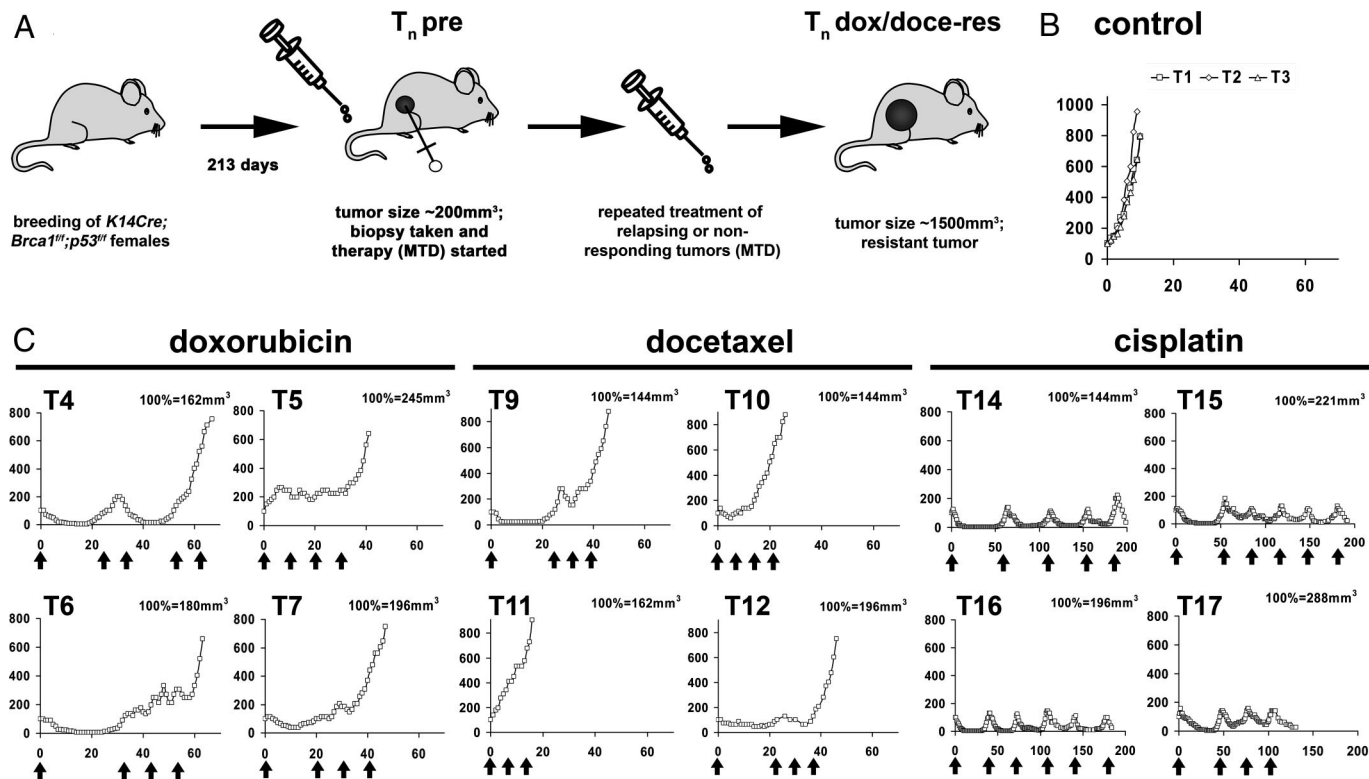


**Fig. 1.** Chemotherapy treatment of mammary tumor-bearing *K14Cre;Brca1<sup>F/F</sup>;p53<sup>F/F</sup>* mice results in resistance to doxorubicin and docetaxel but not to cisplatin. (A) Schematic overview of therapeutic intervention studies in female mice with spontaneous *Brca1<sup>-/-</sup>;p53<sup>-/-</sup>* mammary tumors. (B and C) Tumor-bearing animals (T1–T18) were either left untreated (B) or treated with doxorubicin (5 mg/kg i.v.), docetaxel (25 mg/kg i.v.), or cisplatin (6 mg/kg i.v.), as indicated by the arrows (C). Curves are represented as relative tumor volume ( $0.5 \times \text{length} \times \text{width}^2$ , y axis) over time (days, x axis) and show examples of various responses to drug treatment observed.

marked differences in response among individual tumors, reflecting the intrinsic heterogeneity of spontaneous tumors in the *K14Cre;Brca1<sup>F/F</sup>;p53<sup>F/F</sup>* mouse model. Eventually, however, all tumors became completely resistant to the MTD of doxorubicin or docetaxel. In contrast, we were unable to induce complete resistance to cisplatin. The tumors responded well to this drug but remained sensitive even after five relapses.

**Spontaneous and Orthotopically Transplanted Tumors Show Similar Responses to Anticancer Drugs.** In an attempt to make the model more convenient for tumor intervention studies, we tested whether the tumors could be transplanted orthotopically without losing their morphologic and biochemical properties. Grafting of small tumor pieces (1–2 mm in diameter) from four individual tumors into the fourth right mammary fat pad of syngeneic WT mice resulted in the growth of new tumors after a latency of  $\approx 4$  weeks (tumor volume 150–250 mm<sup>3</sup>). These tumors showed the same histomorphologic features as the original neoplasm (SI Fig. 6B) and the same response to drugs, including inescapable resistance to doxorubicin and docetaxel and repeated response to cisplatin (SI Fig. 6C). Overall, in comparison to doxorubicin and docetaxel, cisplatin treatment significantly increased the median survival ( $P < 0.0002$ ) and the time before relapse after the first treatment ( $P < 0.0007$ ) (SI Fig. 7).

For the use of tumor allografts in drug testing, it was important to test whether different samples of the same tumor responded similarly to chemotherapy. We therefore grafted small tumor pieces (1–2 mm in diameter) of tumor 23 (T23) orthotopically into five syngeneic WT animals, treated four of these with doxorubicin, and left one untreated (SI Fig. 8A and B). The different tumor samples responded similarly after the first treatment with doxorubicin, but the relapsed tumors differed in

their response to additional treatments. These differences in response suggest some regional heterogeneity of the tumor cell population in the original tumor. This heterogeneity is limited, as shown by the gene expression profiles presented below.

Resistance to doxorubicin was not due to altered drug disposition in the host, because most doxorubicin-resistant tumors remained resistant when transplanted into new mice that had not been treated with drug before (SI Fig. 8C). In line with this, the area under the curve for plasma doxorubicin was unaltered after repeated doxorubicin dosing in nontumor-bearing mice (data not shown).

**Frequent Overexpression of *Mdr1a* and/or *Mdr1b* in Doxorubicin-Resistant Tumors.** To further characterize the primary and drug-resistant *Brca1<sup>-/-</sup>;p53<sup>-/-</sup>* mammary tumors, we performed gene expression analyses on 13 doxorubicin-resistant tumors, 8 docetaxel-resistant tumors, and 23 samples from untreated tumors (pretreatment and untreated controls). We used 31,769 oligonucleotide microarrays with reference RNA obtained from a pool of p53-deficient mouse mammary carcinomas (17). Unsupervised hierarchical cluster analysis of the complete data set showed clear coclustering of tumors derived from the same parental tumor (Fig. 2). Individual tumors therefore appear to acquire an individual gene expression fingerprint as they arise, and they largely retain this fingerprint, not only after orthotopic transplantation but also when subjected to additional selection during drug treatment.

We next explored mechanisms of doxorubicin resistance by significance analysis of microarrays (SAM; SI Fig. 9). Comparison of 13 doxorubicin-resistant and 14 untreated tumors ( $\Delta$ , 0.865; false discovery rate, 1.95%) revealed 45 significantly up-regulated genes (SI Table 1). Of these, only the ABC transporter gene *Abcb1a/Mdr1a*, also known as *Mdr3* (20), and a homolog of the human *MDR1* gene, which encodes P-glycoprotein (2), could be function-

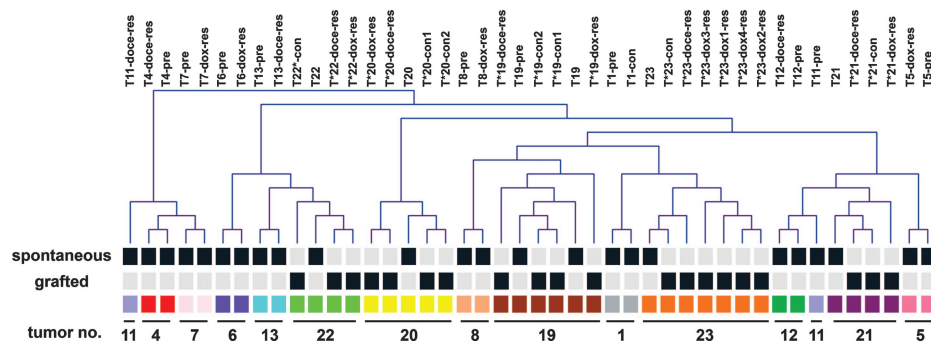


**Fig. 2.** Gene expression fingerprints of individual *Brca1*<sup>-/-</sup>;*p53*<sup>-/-</sup> mammary tumors are retained during chemotherapy treatment. Unsupervised hierarchical cluster analysis of gene expression data showing coclustering of samples derived from the same parental tumor. Amplified RNA (aRNA) from indicated tumor samples and common reference aRNA were fluorescently labeled and cohybridized to mouse 31,769 oligonucleotide microarrays. Samples derived from a single tumor are marked with the same color and black squares indicate whether the tumor was grafted or of spontaneous origin.

ally linked to chemotherapy resistance. By using this approach, we did not find any significantly down-regulated genes and notably no decrease in expression of *topoisomerase II*, which can cause doxorubicin resistance. We also did not observe any significantly altered expression of genes that might alter cell death pathways. Most of the up-regulated genes detected seem to belong to the stromal compartment, because they are either leukocyte-specific or relate to the extracellular matrix. Indeed, more macrophages were present in doxorubicin-resistant tumors, compared with untreated tumors (SI Fig. 10). Possibly, these are secondary effects, e.g., remaining macrophages that removed debris of initial therapy-sensitive cells.

To measure more precisely the expression levels of ABC transporters and other selected genes that might be involved in anticancer drug resistance (SI Table 2), we developed a mouse-specific reverse transcriptase-multiplex ligation-dependent probe amplification (RT-MLPA) mix and tested it on our panel of drug-sensitive and -resistant tumor samples (Fig. 3 and SI Table 3). For normalization of expression levels, we used two

internal references, *Actinβ*, a small mRNA (1,892 nt), and *Mrp1*, a large mRNA (5,944 nt). Although human MRP1 transports anthracyclines, the murine *Mrp1* does not (21). In line with this, *Mrp1* was not up-regulated in any of the doxorubicin-resistant tumors. Comparison of the expression levels of the selected genes in the resistant and sensitive tumor samples, showed that only *Mdr1a* and *Mdr1b* were significantly up-regulated in a substantial fraction of the doxorubicin-resistant tumors (Fig. 3 and SI Table 3). In different resistant tumors, the levels differed between 2.5- and 90-fold. Only 2 of 13 doxorubicin-resistant tumors (T\*21-dox-res and T\*23-dox1-res) showed no change in the expression of *Mdr1a* and *Mdr1b*. *Bcrp1* expression was increased 5-fold in T4-dox-res and  $\geq 2$ -fold in two other tumors (T6-dox-res and T8-dox-res). No significant decrease of *topoisomerase II* expression was detected in any of the doxorubicin-resistant tumors. Similarly, gene expression levels of *Parp1* and *Parp2* (DNA repair) (22); *CD24*, *CD29*, and *CD49f* (breast stem cell markers) (23, 24); and *Hsp90* did not show noticeable differences.

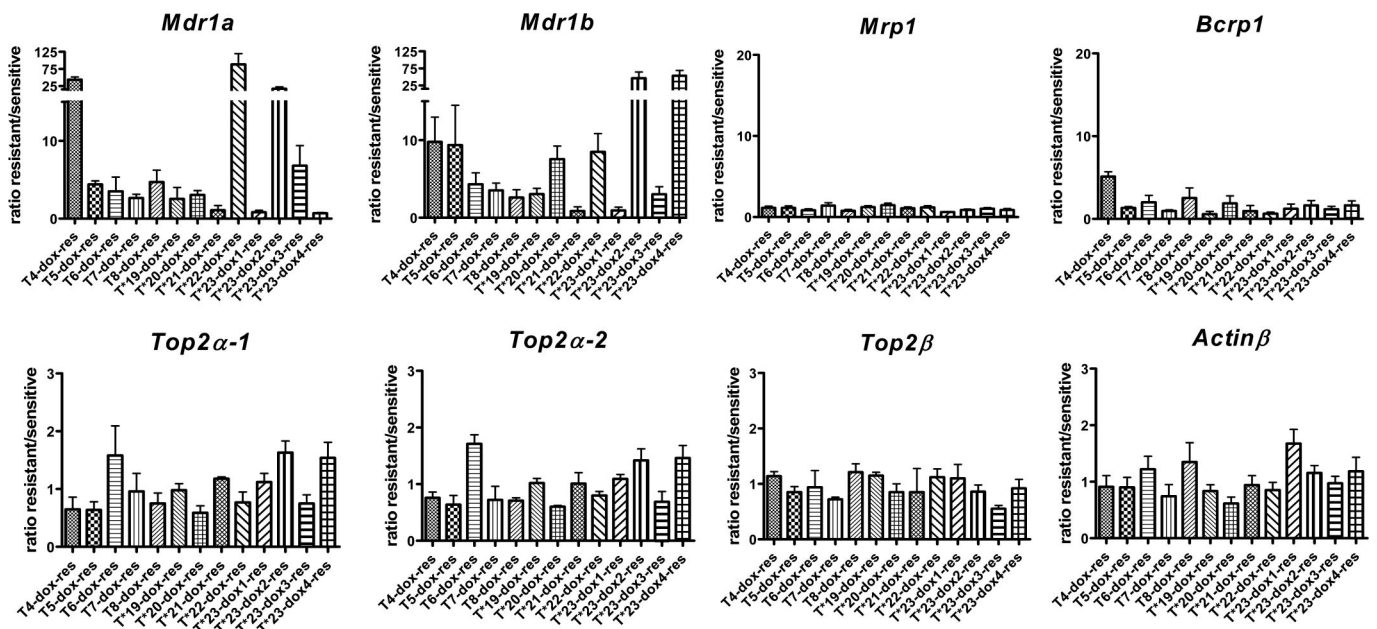


**Fig. 3.** Expression of *Mdr1a*, *Mdr1b*, and other selected genes in doxorubicin-sensitive and -resistant tumors. Ratios of gene expression in doxorubicin-resistant tumors and samples from the corresponding drug-sensitive tumors before treatment. Shown are RT-MLPA analyses of 13 doxorubicin-resistant tumors. The sum of the values for *Actinβ* and *MRP1* was used as internal reference for *Mdr1a*, *Mdr1b*, *Bcrp1*, *Top2α* (two different sequences targeted), and *Top2β*. *MRP1* was compared with *Actinβ* and vice versa. The presented values represent the mean ratio of three independent reactions. Error bars indicate standard deviation. For the complete data set, see SI Table 3.



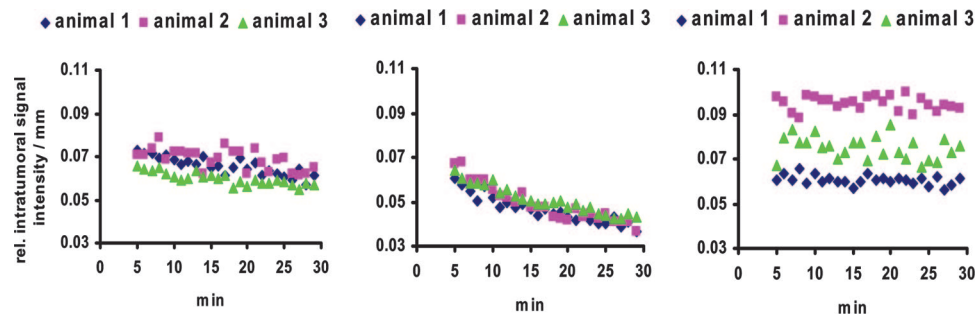


**Fig. 4.** Functional imaging of doxorubicin-resistant tumors shows increased drug transporter activity *in vivo*. Nuclear imaging was used to measure  $^{99m}\text{Tc}$ -sestamibi uptake and washout in a doxorubicin-sensitive tumor (T\*23-con) (Left) and a doxorubicin-resistant tumor (T\*23-dox2-res), with (Right) or without (Center) pretreatment of the Mdr1a/Mdr1b inhibitor cyclosporin A.

We have analyzed the P-glycoprotein content of the doxorubicin-resistant tumors by using the C219 monoclonal antibody routinely used to detect human and mouse P-glycoproteins (25, 26). Whereas we readily detected increased P-glycoprotein levels in resistant tumors (T4-dox-res, T5-dox-res, T7-dox-res, T\*20-dox-res, T\*22-dox-res, T\*23-dox2-res, and T\*23-dox4-res) on Western blots, we were unable to detect the protein by immunohistochemistry in these tumors under conditions that allowed simple detection of P-glycoprotein in mouse liver or in transfected cells overexpressing *MDR1*, *Mdr1a*, or *Mdr1b* (data not shown). This suggests that current methods fail to detect low P-glycoprotein levels that contribute to drug resistance, and we are investigating this issue using P-glycoprotein inhibitors.

**Doxorubicin-Resistant Tumors Show Cross-Resistance to Docetaxel.** A hallmark of doxorubicin resistance mediated by P-glycoprotein is cross-resistance to taxanes, because other biochemical doxorubicin resistance mechanisms do not affect taxane sensitivity. We transplanted pieces of four individual doxorubicin-resistant tumors (T\*23-dox1-res, T\*23-dox2-res, T\*23-dox3-res, and T\*23-dox4-res) orthotopically into the fourth right mammary fat pad of WT animals and treated the tumor with docetaxel or cisplatin (SI Fig. 11B). Whereas a graft from the primary tumor showed clear growth retardation in response to docetaxel (SI Fig. 11A), the doxorubicin-resistant tumors T\*23-dox2-res, T\*23-dox3-res, and T\*23-dox4-res were completely cross-resistant to the P-glycoprotein substrate docetaxel. These are tumors with an increased *Mdr1a* and/or *Mdr1b* expression (Fig. 3 and SI Table 3). In contrast, tumor T\*23-dox1-res, in which no *Mdr1a/Mdr1b* up-regulation was detected, and which also showed delayed doxorubicin resistance after transplantation (SI Fig. 8C), remained initially sensitive to docetaxel (SI Fig. 11B). All tumors were still sensitive to cisplatin, showing that cisplatin-induced cell death was not affected by the mechanism of doxorubicin resistance.

**Doxorubicin-Resistant Tumors Show Increased Drug Extrusion *in Vivo*.** P-glycoprotein transports substrate drugs out of tumor cells once they get in. This can be visualized *in vivo* by measuring tumor uptake and washout of the Mdr1a/Mdr1b substrate  $^{99m}\text{Tc}$ -sestamibi (27). To test this with our *Brcal1*<sup>-/-</sup>; *p53*<sup>-/-</sup> tumors, fragments of the doxorubicin-resistant tumor T\*23-dox2-res were transplanted orthotopically into the fourth right mammary fat pad of six WT mice. As a control, fragments of the doxorubicin-sensitive tumor T23 were transplanted into three animals. When tumors reached a size of  $\approx 1\text{ cm}^3$ ,  $^{99m}\text{Tc}$ -sestamibi was injected i.v., and  $^{99m}\text{Tc}$ -sestamibi efflux from the tumor was monitored by a gamma camera between 5 and 30 min after injection (Fig. 4). Three of the mice engrafted with the doxorubicin-resistant tumor T\*23-dox2-res were treated with the Mdr1a/Mdr1b/P-glycoprotein inhibitor cyclosporin A (28) before  $^{99m}\text{Tc}$ -sestamibi injection and imaging. After 30 min, the  $^{99m}\text{Tc}$ -sestamibi concentration had decreased by  $\approx 12\%$  in the

control tumors but by 35% in the doxorubicin-resistant tumors. Pretreatment of the doxorubicin-resistant tumor with cyclosporin A reduced  $^{99m}\text{Tc}$ -sestamibi efflux to 2% over a 30-min period. These results are compatible with a resistance mechanism due to increased efflux of drug, e.g., by P-glycoprotein.

## Discussion

We have found that resistance against doxorubicin and docetaxel can be readily induced in the *Brcal1*<sup>-/-</sup>; *p53*<sup>-/-</sup> tumors that we have studied. The resistance is clinically relevant, at least in mice, because the mice are treated with the MTD of drugs. Such a mouse model of anticancer drug resistance has not been reported before, either for transplantable mouse tumors or for human xenografts. We think that “spontaneous” tumors may get the chance to become drug resistant, because they are not immunogenic, but direct evidence is lacking for this speculation.

Although a complete analysis of all resistant tumors remains to be done, our partial analysis has already yielded clear results regarding the pathways that cause drug resistance in *Brcal1*<sup>-/-</sup>; *p53*<sup>-/-</sup> tumors. Most importantly, we find no indication that blocks in apoptosis and/or senescence play a crucial role in causing resistance. We have not found significant changes in the expression of genes involved in apoptosis, such as *Bcl2*, *Apaf1*, or caspase genes. Moreover, we have been unable to induce resistance against cisplatin treatment, which should occur if interference with cell death pathways would be an option for generating generalized drug resistance in these tumors. The major resistance mechanism identified thus far is up-regulation of the *Mdr1a* and *Mdr1b* murine P-glycoprotein genes, which occurs in the majority of doxorubicin-resistant tumors. Semiquantitative expression analysis by RT-MLPA has shown for some tumors that up-regulation is substantial, up to 90-fold. This should be sufficient for an MDR phenotype and, indeed, we found cross-resistance between two drugs with very different chemical structures and cellular targets, doxorubicin (an anthracycline that targets topoisomerase II) and docetaxel (a taxane that targets tubulin), in the tumors for which this was tested. Both drugs are good substrates for P-glycoprotein (2). Moreover, we found increased efflux of the P-glycoprotein substrate  $^{99m}\text{Tc}$ -sestamibi in one of the tumors with high P-glycoprotein levels, supporting the relevance of P-glycoprotein in causing *in vivo* drug resistance.

In preliminary experiments, we have seen that both tumors with high (90-fold) and low (5-fold) *Mdr1a/Mdr1b* overexpression respond again to doxorubicin in combination with the specific P-glycoprotein blocker tariquidar (Avaant Pharma, London, U.K.), confirming the relevance of moderate increases of P-glycoprotein in drug resistance developing *in vivo* (data not shown).

Our results are fundamentally different from those reported by Schmitt, Lowe, and coworkers for p53-proficient lymphomas from *E $\mu$ -myc* transgenic mice (29–31). The *E $\mu$ -myc* lymphoma cells were

found to be sensitive to any cytotoxic treatment and readily underwent apoptosis when challenged (29). Relapsing tumors acquired resistance to doxorubicin and cyclophosphamide (32). Interfering with apoptosis (by *Bcl-2* or *Akt* overexpression) or senescence (by *p53* or *Ink4a* mutation) or both resulted in diminished efficacy of a single dose of cyclophosphamide, and therefore blocks in apoptosis/senescence pathways can contribute to primary resistance in the *Eμ-myc* model (31, 33, 34).

In contrast, the tumors that we study here are derived from epithelial cells, as are >90% of human cancers, and they lack a functional *p53* pathway, like most human tumors (13). Obviously, inactivating apoptotic/senescence pathways is not a readily available mechanism for resistance in these mammary tumors. We consider this an important conclusion, given the current preoccupation with blocks in apoptosis/senescence as a major mechanism of MDR of tumors (7). This does not mean that loss of components of the apoptotic pathway could not play a role in the MDR phenotype of some tumors of epithelial origin. Indeed, there is evidence that a decrease in Apaf-1 could contribute to therapy resistance of melanomas (35). That blocks in apoptosis/senescence can contribute to chemotherapy resistance of lymphomas/leukemias is not in dispute and is also supported by recent work on other mouse models (36, 37).

With cisplatin, we were unable to get resistance, but nevertheless, we were also unable to eradicate the tumors, which invariably regrew from the small tumor remnants remaining after treatment. These “remnants” might have special properties rendering the tumor cells insensitive to the cisplatin. These cells could be poorly accessible to drug or could represent a noncycling subpopulation. It is tempting to think, however, that the remnants consist of tumor-initiating cells with stem cell-like properties that are resistant to cisplatin but become sensitive after differentiation.

That the “spontaneous” mouse mammary tumors in our *K14cre;Brca1<sup>F/F</sup>;p53<sup>F/F</sup>* model resemble the natural history of human tumors is an advantage but comes at a cost: each mammary tumor that spontaneously arises in our mice has accumulated different mutations in the period between the initiating deletions of *Brca1/p53* and the final tumor. This pronounced individuality is obvious from the differential response to drugs and from the differences in gene expression profiles. Nevertheless, the tumors share certain basic properties, i.e., growth inhibition by the three drugs tested, sensitivity to cisplatin, and ability to become resistant to doxorubicin and docetaxel but not to cisplatin.

How relevant are our results for interpreting the effects of chemotherapy on human cancer? The only resistance mechanism that we have thus far found to be regularly associated with doxorubicin resistance in the mouse mammary tumors is up-regulation of the *Mdr1a* and *Mdr1b* genes. The possible involvement of its human counterpart, *MDR1*, in human breast cancer is still controversial (38). Nevertheless, we think that the “spontaneous” mouse models have potential for drug studies relevant to human chemotherapy. The opportunities that genetically engineered mice offer in cancer drug development are manifold (39). There are never enough human patients to optimize drug combinations/schedules and, with a large number of new drugs in development, better animal models to test possible new treatment combinations should be useful. Indeed, the high sensitivity of our *Brca1*-deficient mouse mammary tumors to cisplatin is of interest against the background of ongoing trials in human breast cancer patients that attempt to exploit the defective DNA repair of these tumors by targeting DNA with platinum drugs. In an attempt to develop treatment capable of eradicating *Brca1<sup>-/-</sup>;p53<sup>-/-</sup>* mammary tumors, we have started experiments in which treatment with cisplatin or carboplatin is combined with a previously undescribed drug that targets BRCA-deficient cells through inhibition of PolyADP-Ribose Polymerase 1 (40, 41).

## Materials and Methods

**Animals, Generation of Mammary Tumors, and Orthotopic Transplantations into Syngeneic WT Mice.** *Brca1<sup>-/-</sup>;p53<sup>-/-</sup>* mammary tumors were generated in *K14cre;Brca1<sup>F/F</sup>;p53<sup>F/F</sup>* mice and genotyped as described by Liu *et al.* (17) and Jonkers *et al.* (42). In these animals, the onset of tumor growth was checked at least three times per week from the age of 4 months onward. Mammary tumor size was determined by caliper measurements (length and width in millimeters), and tumor volume ( $\text{mm}^3$ ) was calculated by using the following formula:  $0.5 \times \text{length} \times \text{width}^2$ . For orthotopic transplantations, small tumor fragments (1–2 mm in diameter, mechanically minced in ice-cold PBS) were grafted into the mammary fat pad of female WT (FVB/n  $\times$  129/Ola)F<sub>1</sub> animals (6–12 weeks of age). For this purpose, animals were anesthetized with hypnorm/dormicum/H<sub>2</sub>O (1:1:2, 7 ml/kg), and a small abdominal skin incision was made to explore the fourth right mammary gland fat pad with watchmaker forceps. With the latter, a small pocket was generated in the fat pad into which a tumor piece was installed. After postoperative surveillance (including s.c. injection of 0.1 mg of buprenorphin per kilogram), tumor growth was controlled at least three times per week starting 2 weeks after transplantation. Animals were killed with CO<sub>2</sub> when the tumor volume reached 1,500  $\text{mm}^3$ . In addition to sterile collection of multiple tumor pieces for grafting experiments ( $\approx 30\%$  of total volume), tumor samples were snap-frozen in liquid nitrogen, fixed in both 4% formaline and acetic acid-formaline ethanol-saline (43), and embedded in Tissue-Tek Optical Cutting Temperature (OCT). All experimental procedures on animals were approved by the Animal Ethics Committee of the Netherlands Cancer Institute.

**Drugs.** Doxorubicin [Adriablastina (40:5:10:45 v/v); Amersham Pharmacia Netherlands, Woerden, The Netherlands] was diluted to 1 mg/ml in saline (Braun, Emmer-Compascuum, The Netherlands). Docetaxel (Taxotere, 10 mg/ml in Tween80/ethanol/saline 20:13:67 vol/vol/vol; Aventis, Antony Cedex, France) was diluted with saline to 5 mg/ml before injection. Cisplatin (1 mg/ml in saline-mannitol) originated from Mayne Pharma (Brussels, Belgium). Cyclosporin A (Sandimmune, 50 mg/ml in cremophor EL-ethanol 67:33, vol/vol; Novartis, Basel, Switzerland) was diluted to 5 mg/ml in saline before injection.

**Treatment of Mammary Tumor-Bearing Animals.** When *Brca1<sup>-/-</sup>;p53<sup>-/-</sup>* mammary tumors reached a size of  $\approx 200 \text{ mm}^3$ , animals were anesthetized (methoxyflurane; Medical Developments Australia, Melbourne, Australia), and a tumor biopsy was taken with a 15-gauge trocar and snap-frozen in liquid nitrogen. One to 2 hs after anesthesia recovery, doxorubicin (5 mg/kg), docetaxel (25 mg/kg), or cisplatin (6 mg/kg) was injected i.v. After the initial treatment, tumor size was determined at least three times per week. Based on SI Fig. 5, a recovery time of 7 (docetaxel), 10 (doxorubicin), and 20 days (cisplatin) was given before additional treatments. To avoid accumulating toxicity of repeated injections, an additional treatment was not given after the recovery time when the tumor responded to the treatment (tumor size <50% of the original volume, partial response). In that case, treatment was continued once the tumor relapsed to its original size (100%). For tumors with a volume  $\geq 50\%$  after the recovery time, an additional treatment with the same dose as mentioned above was given. For WT animals harboring grafted tumors, a recovery time of 7 days was used for all drugs.

**RNA Extraction, Amplification, and Microarray Hybridization.** From the snap-frozen tumor samples, total RNA was isolated, and polyA<sup>+</sup> RNA was amplified, labeled, and hybridized as described by Liu *et al.* (17). The complete protocols for RNA amplification, labeling, and microarray hybridizations can be found on <http://microarrays.nki.nl/download/protocols.html>. All experiments were



performed as fluorochrome-reversed two-color duplicate hybridizations on mouse microarrays (Central Microarray Facility, NKI Amsterdam, Amsterdam, The Netherlands) containing 31,769 70-mer probes representing 18,173 genes and 32,829 gene transcripts (Operon Biotechnologies, Huntsville, AL). Hybridized slides were scanned on a Agilent Microarray Scanner, analyzed by using ImaGene software (BioDiscovery, El Segundo, CA), and uploaded into our database, where a Lowess normalization is automatically performed.

**Processing of Microarray Data.** After data normalization (44), a modified Rosetta error model (45) was used on the fluorochrome-reversed two-color duplicates to calculate the average ratio per gene and a *P* value indicating the chance a gene is falsely classified. All probes with significant changes in expression ( $\log_2 \text{ratio} > 1$  or  $< -1$ ) in  $< 10\%$  of the samples were filtered out. Also probes with missing data points in more than 10% of the hybridizations were excluded.

**Unsupervised Hierarchical Clustering and SAM.** The TIGR Multiexperiment Viewer 3.1 software (TMV3.1, [www.tm4.org/mev.html](http://www.tm4.org/mev.html)) was used to perform both unsupervised hierarchical clustering and SAM analysis. The unsupervised 1D hierarchical clustering algorithm was based on Euclidean distance, and complete linkage and was applied to group tumor samples according to similarity in the pattern of gene expression. SAM analysis was performed to identify genes that were significantly changed in 13 doxorubicin-resistant tumors vs. nontreated samples from 14 individual tumors.

**RT-MLPA Analysis.** Synthetic MLPA probes consisting of either two or three oligonucleotides were developed as described (46). All MLPA probes were designed to span an intron to reduce DNA-generated background. In addition, a specific reverse transcription primer was developed for each probe. To reduce endogenous expression levels, a specific ratio of competitor probe (lacking the 5' primer sequence) was included. A list of all MLPA probes, reverse transcription primers and the ratio of competitor probes to MLPA probes can be found in **SI Table 2**. Hybridization, ligation, PCR amplification, and fragment analysis by capillary electrophoresis were performed as described (47).

**Histology.** Tissues were fixed in 4% formaldehyde or EAFS (43) overnight, embedded in paraffin, and cut at 4- $\mu\text{m}$  sections. After

deparaffinization and rehydration, sections were stained with H&E.

**In Vivo Imaging.** Anesthetized mice were immobilized on a Plexiglass plate and examined by using x-ray and gamma imaging. A conventional mammography unit (Selenia, Lorad, Danbury, CT) was used for x-ray imaging at 25 kV and 85 mAs. In three animals, 50 mg of cyclosporin A per kilogram of body weight was injected i.v. 1 h before gamma imaging. For the gamma imaging, 30 MBq ( $\approx 100 \mu\text{l}$ ) of the P-glycoprotein substrate  $^{99\text{m}}\text{Tc}$ -Sestamibi was administered i.v., followed by the acquisition of 25 consecutive gamma images, each at 1-min acquisition time. All images were obtained by using a conventional gamma camera (Argus ZQ04; Philips, Eindhoven, The Netherlands) at identical settings. Three  $^{57}\text{Co}$  markers were attached to the Plexiglas plate to allow spatial alignment of x-ray and gamma images by using customized image fusion software (**SI Fig. 12**). The  $^{99\text{m}}\text{Tc}$ -sestamibi washout was quantified in all animals by placing a six-pixel region of interest (ROI) in the tumor guided by the x-ray image. In each gamma image, the relative signal in the tumor was defined as:  $I_{\text{rel tumor}}(t) = [(S_{\text{tumor}}(t)/W_{\text{tumor}})/S_{\text{mouse}}(t)] \times 100\%$ , where  $S_{\text{tumor}}(t)$  indicates the total image intensity in the ROI at time *t*;  $W_{\text{tumor}}$ , the width of the tumor in millimeters; and  $S_{\text{mouse}}(t)$ , the total image intensity at time *t* in the mouse, including surrounding scatter field but excluding the tail section. The relative signal was normalized to the width of the tumor to compensate for differences in gamma signal because of differences in tumor thickness.

We thank the technical staff of the NKI-AvL animal facility (in particular T. Maidment) for expert assistance in animal care; R. Kerkhoven, M. Heimerikx, and A. Velds for help with microarray hybridizations and analysis; R. Valdés Olmos, B. Pool, L. Rooze, and C. Feenstra from the Nuclear Medicine Department and W. Hoogbeem from the Department of Radiology for assistance in the *in vivo* imaging; and R. Bernards, A. Berns, M. van Lohuizen, H. te Riele, L. Wessels, and M. van de Vijver for helpful comments on the manuscript. Financial support for this work came from the Dutch Cancer Society (Grant NKI 2001-2473, to P.B. and J. Wijnholds; Grant NKI 2002-2635, to J.J. and A. Berns; Grant NKI 2005-3379 to P.B., R. Bernards, and R. L. Beijersbergen; and Grant NKI 2006-3566, to P.B., S.R., and J.J.). S.R. was supported by fellowships from the Swiss National Science Foundation (PBBEB-104429) and the Swiss Foundation for Grants in Biology and Medicine, and F.W.B.v.L. is supported by the Technology Foundation STW (Veni Grant BGT 7528).

1. Gottesman MM (2002) *Annu Rev Med* 53:615–627.
2. Szakacs G, Paterson JK, Ludwig JA, Booth-Gentle C, Gottesman MM (2006) *Nat Rev Drug Discov* 5:219–234.
3. Gorre ME, Mohammed M, Ellwood K, Hsu N, Paquette R, Rao PN, Sawyers CL (2001) *Science* 293:876–880.
4. *Cancer, Principles and Practice of Oncology* (2001), eds De Vita VT, Hellman S, Rosenberg SA (Lippincott Williams & Wilkins, Philadelphia).
5. Shabbits JA, Hu Y, Mayer LD (2003) *Mol Cancer Ther* 2:805–813.
6. Voorzanger-Rousselot N, Alberti L, Blay JY (2006) *BMC Cancer* 6:75.
7. Debatin KM (2004) *Cancer Immunol Immunother* 53:153–159.
8. Minchinton AI, Tannock IF (2006) *Nat Rev Cancer* 6:583–592.
9. Borst P, Borst J, Smets LA (2001) *Drug Resist Updat* 4:129–131.
10. Borst P, Rottenberg S (2005) *Drug Resist Updates* 7:321–324.
11. Schmitt CA, Lowe SW (2001) *Drug Resist Updates* 4:132–134.
12. Brown JM, Wilson G (2003) *Cancer Biol Ther* 2:477–490.
13. Brown JM, Attardi LD (2005) *Nat Rev Cancer* 5:231–237.
14. Finkel E (1999) *Science* 286:2256–2258.
15. Roninson IB, Broude EV, Chang B-D (2001) *Drug Resist Updates* 4:303–313.
16. Jonkers J, Berns A (2005) in *Introduction to the Cellular and Molecular Biology of Cancer*, eds Knowles M, Selby P (Oxford University, Oxford, UK), pp 317–336.
17. Liu A, Holstege H, van der Gulden H, Treur-Mulder M, Zevenhoven MJ, Velds A, Kerkhoven RM, van Vliet MH, Wessels LFA, Peterse JL, et al. (2007) *Proc Natl Acad Sci USA* 104:12111–12116.
18. Bhattacharyya A, Ear US, Koller BH, Weichselbaum RR, Bishop DK (2000) *J Biol Chem* 275:23899–23903.
19. Tassone P, Tagliaferri P, Perricelli A, Blotta S, Quaresima B, Martelli ML, Goel A, Barbieri V, Costanzo F, Boland CR, et al. (2003) *Br J Cancer* 88:1285–1291.
20. Raymond M, Rose E, Housman DE, Gros P (1990) *Mol Cell Biol* 10:1642–1651.
21. Stride BD, Grant CE, Loe DW, Hipfner DR, Cole SPC, Deeley RG (1997) *Mol Pharmacol* 52:344–353.
22. D'Amours D, Desnoyers S, D'Silva I, Poirier GG (1999) *Biochem J* 342:249–268.
23. Stingl J, Eirew P, Ricketson I, Shackleton M, Vaillant F, Choi D, Li H, Eaves CJ (2006) *Nature* 439:993–997.
24. Shackleton M, Vaillant F, Simpson KJ, Stingl J, Smyth GK, Asselin-Labat ML, Wu L, Lindeman GJ, Visvader JE (2006) *Nature* 439:84–88.
25. Barrand MA, Twentyman PR (1992) *Br J Cancer* 65:239–245.
26. Chintamani, Singh JP, Mittal MK, Saxena S, Bansal A, Bhatia A, Kulshreshtha P (2005) *World J Surg Oncol* 3:61.
27. Tatsumi M, Tsuruo T, Nishimura T (2002) *Eur J Nucl Med Mol Imaging* 29:288–294.
28. Leonard GD, Fojo T, Bates SE (2003) *Oncologist* 8:411–424.
29. Schmitt CA, Rosenthal CT, Lowe SW (2000) *Nat Med* 6:1029–1035.
30. Schmitt CA, Fridman JS, Yang M, Baranov E, Hoffman RM, Lowe SW (2002) *Cancer Cell* 1:289–298.
31. Schmitt CA, Fridman JS, Yang M, Lee S, Baranov E, Hoffman RM, Lowe SW (2002) *Cell* 109:335–346.
32. Schmitt CA, Wallace-Brodeur RR, Rosenthal CT, McCurrach ME, Lowe SW (2000) *Cold Spring Harb Symp Quant Biol* 65:499–510.
33. Schmitt CA, McCurrach ME, de Stanchina E, Wallace-Brodeur RR, Lowe SW (1999) *Genes Dev* 13:2670–2677.
34. Wendel HG, de Stanchina E, Fridman JS, Malina A, Ray S, Kogan S, Cordon-Cardo C, Pelletier J, Lowe SW (2004) *Nature* 428:332–337.
35. Soengas MS, Gerald WL, Cordon-Cardo C, Lazebnik Y, Lowe SW (2006) *Cell Death Differ* 13:352–353.
36. Wendel HG, de Stanchina E, Cepero E, Ray S, Emig M, Fridman JS, Veach DR, Bornmann WG, Clarkson B, McCombie WR, et al. (2006) *Proc Natl Acad Sci USA* 103:7444–7449.
37. Williams RT, Roussel MF, Sherr CJ (2006) *Proc Natl Acad Sci USA* 103:6688–6693.
38. O'Driscoll L, Clynes M (2006) *Curr Cancer Drug Targets* 6:365–384.
39. Sharpless NE, DePinho RA (2006) *Nat Rev Drug Discov* 5:741–754.
40. Farmer H, McCabe N, Lord CJ, Tutt AN, Johnson DA, Richardson TB, Santarosa M, Dillon KJ, Hickson I, Knights C, et al. (2005) *Nature* 434:917–921.
41. Bryant HE, Schultz N, Thomas HD, Parker KM, Flower D, Lopez E, Kyle S, Meuth M, Curtin NJ, Helleday T (2005) *Nature* 434:913–917.
42. Jonkers J, Meuwissen R, van der Gulden H, Peterse H, Van der Valk M, Berns A (2001) *Nat Genet* 29:418–425.
43. Harrison PT (1984) *Lab Anim* 18:325–331.
44. Yang YH, Dudoit S, Luu P, Lin DM, Peng Y, Ngai J, Speed TP (2002) *Nucleic Acids Res* 30:e15.
45. Weng L, Dai H, Zhan Y, He Y, Stepaniants SB, Bassett DE (2006) *Bioinformatics* 22:1111–1121.
46. Langerak P, Nygren AO, Schouten JP, Jacobs H (2005) *Nucleic Acids Res* 33:e188.
47. Schouten JP, McElgunn CJ, Waaijer R, Zwijnenburg D, Diepvens F, Pals G (2002) *Nucleic Acids Res* 30:e57.